

Polarimetry with Phased Array Antennas: Sensitivity and Polarimetric Performance Using Unpolarized Sources for Calibration

Stefan J. Wijnholds *Senior Member, IEEE*, Marianna V. Ivashina *Member, IEEE*, Rob Maaskant *Member, IEEE*, Karl F. Warnick *Senior Member, IEEE*

Abstract—Polarimetric phased arrays require a calibration method that allows the system to measure the polarization state of the received signals. In this paper, we assess the polarimetric performance of two commonly used calibration methods that exploit unpolarized calibration sources. The first method obtains a polarimetrically calibrated beamforming solution from the two dominant eigenvectors of the measured signal covariance matrix. We demonstrate that this method is sensitivity equivalent to the theoretical optimal method, but suffers from an ambiguity that has to be resolved by additional measurements on (partially) polarized sources or by exploiting the intrinsic polarimetric quality of the antenna system. The easy-to-implement bi-scalar approach assumes that the feed system consists of two sets of orthogonally oriented antenna elements, each associated with one polarization. We assess its sensitivity and polarimetric performance over a wide field-of-view (FoV) using simulations of a phased array feed system for the Westerbork Synthesis Radio Telescope. Our results indicate that the sensitivity loss can be limited to 4.5% and that the polarimetric performance over the FoV is close to the best achievable performance. The latter implies that the intrinsic polarimetric quality of the antennas remains a crucial factor despite the development of novel polarimetric calibration methods.

Index Terms—phased array antennas, polarimetry, calibration, beamforming, far-field radiation pattern

I. INTRODUCTION

Polarimetric phased array antenna systems are commonly used in imaging radar applications [1], [2], but are relatively new in the field of radio astronomy. The radio astronomical community is developing the Square Kilometre array (SKA) [3], a future radio telescope that is envisaged to be an order of magnitude more sensitive than present-day instruments. Phased array antennas will play a crucial role either as aperture array (AA) or as phased array feed (PAF) for reflector antennas. Several precursor and pathfinder systems using phased array antennas are currently in use or being developed. Examples of such instruments are the Low Frequency Array (LOFAR, AA) in Europe [4], the aperture tile-in-focus (APERTIF, PAF)

S.J. Wijnholds is with the Netherlands Institute for Radio Astronomy (ASTRON), P.O. Box 2, NL-7990 AA, Dwingeloo, The Netherlands, Email: wijnholds@astron.nl

M.V. Ivashina is with Chalmers University of Technology, SE-412 96 Gothenburg, Sweden and with the Netherlands Institute for Radio Astronomy (ASTRON), Email: ivashina@chalmers.se

R. Maaskant is with Chalmers University of Technology, Email: maaskant@chalmers.se

K.F. Warnick is with the Department of Electrical and Computer Engineering, Brigham Young University, 459 Clyde Building, Provo, UT 84602, USA, Email: warnick@ee.byu.edu

upgrade of the Westerbork Synthesis Radio Telescope in The Netherlands [5], the Australian SKA Pathfinder (ASKAP, PAF) in the Western Australian Desert [6] and the Long Wavelength Array (LWA, AA) in the US [7].

The goals of these instruments for future radio astronomy research require high system sensitivity for detecting weak radio signals and accurate reconstruction of the polarization state of these signals. A polarimetric antenna system, capable of sampling the incident field by two orthogonally polarized receptors, can fully reconstruct the polarization state of the field. This reconstruction can be done by inverting a 2×2 transfer matrix that relates the two output signals of the receiver system to the polarization state of the field received by the system [8]. In polarimetric systems, calibration should not only compensate the gain differences between the receiving elements to provide maximum sensitivity at the beamformer outputs, but also ensure that the covariance between the two beamformer output signals allows proper reconstruction of the polarization state of the incident field. In a recent paper [9], the authors have developed a system model and used it to relate the astronomical performance criteria to standard IEEE definitions for polarimetric antennas and to find a beamforming algorithm that simultaneously optimizes for minimum system noise and polarimetric accuracy. In this paper, we use this framework to assess the polarimetric performance and sensitivity of two commonly used calibration methods that exploit unpolarized sources. This is particularly relevant, because the majority of extragalactic radio sources with a continuum spectrum, which are typically used for calibration of radio telescopes, are weakly polarized or unpolarized and hence calibration methods based on polarized reference sources are usually not applicable.

A recently proposed method exploits the two dominant eigenvectors of the signal covariance matrix measured on an unpolarized source with a dual-polarized array [10], which we will refer to as eigenvector method. This method may cause a large unknown change of the orientation of the polarization axes of the instrument, as we demonstrate in this paper, and is therefore unsuitable for application in actual systems without further polarimetric corrections. These polarimetric corrections either require additional measurements on polarized sources or relying on the intrinsic polarimetric quality of the system.

A second commonly used method exploits the fact that feed systems usually consist of two sets of orthogonally oriented antenna elements. For such systems, it is common

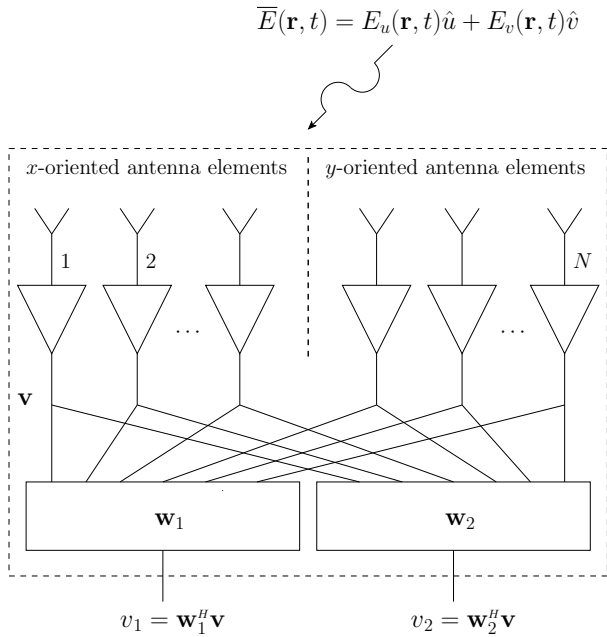


Fig. 1. A radio polarimeter comprised of a dual-polarized actively beamformed receiving antenna array.

practice to calibrate the two sets independently and to apply a single polarization correction at the end. This bi-scalar method imposes additional constraints on the system design, including manufacturing tolerances. We assess the stringency of these constraints by comparison with the theoretically optimal performance using theoretical analysis and simulations.

This paper is organized as follows. We start by introducing the system model and performance metrics used to assess the performance of the antenna system. In Sec. III we introduce the calibration methods and discuss their theoretical performance. We then introduce a simple analytic dipole model in Sec. IV to demonstrate the impact of the unitary ambiguity introduced when calibrating on an unpolarized source and show how the polarimetric quality of the methods exploiting the intrinsic polarimetric quality of the antenna system depends on the orthogonality between the feed systems. In Sec. V, we present simulations for an actual PAF system to assess the impact of using a bi-scalar instead of a full-polarimetric approach on the sensitivity and polarimetric performance over the field-of-view (FoV). We show that the sensitivity loss can be limited to 4.5% while the polarimetric performance over the FoV is comparable to the best achievable performance.

II. THEORY

A. System model

Figure 1 shows an N -element polarimetric phased array. The antenna system is assumed to be illuminated by a partially polarized source. The electric field intensity vector radiated by such a source is

$$\overline{\mathbf{E}}(\mathbf{r}, t) = E_u(\mathbf{r}, t)\hat{u} + E_v(\mathbf{r}, t)\hat{v}, \quad (1)$$

where \hat{u} and \hat{v} are orthogonal unit vectors according to a certain specific Ludwig's definition [11] relative to the coordinate system of the array.

The antenna output signals are amplified to form the N -element output voltage vector \mathbf{v} and are subsequently combined into the beamformer output voltages v_1 and v_2 using the $N \times 1$ beamformer weight vectors \mathbf{w}_1 and \mathbf{w}_2 .

At a fixed position \mathbf{r} , $E_u(\mathbf{r}, t)$ and $E_v(\mathbf{r}, t)$ are complex random processes in the phasor or complex baseband representation. The polarization state of the field is determined by the correlation matrix of the two field components, which is

$$\mathbf{\Sigma} = \begin{bmatrix} \sigma_{uu} & \sigma_{uv} \\ \sigma_{vu} & \sigma_{vv} \end{bmatrix} = \begin{bmatrix} \langle |E_u|^2 \rangle & \langle E_u E_v^* \rangle \\ \langle E_u^* E_v \rangle & \langle |E_v|^2 \rangle \end{bmatrix}, \quad (2)$$

where $\langle \cdot \rangle$ denotes the expected value. For an unpolarized source, we have $\mathbf{\Sigma} = \mathbf{I}$.

We will model the phased array antenna signal output in terms of the voltage response vectors of the array, \mathbf{v}_u and \mathbf{v}_v , containing voltages at the array receiver outputs before beamforming induced by unit intensity, linearly polarized waves having their polarization aligned with \hat{u} and \hat{v} respectively. Theoretically, these voltages can be measured using a reference source producing two signals with perfectly orthogonal polarizations.

For an arbitrary polarized wave, the array signal voltage response vector can be formulated in terms of \mathbf{v}_u and \mathbf{v}_v as

$$\mathbf{v}_s = E_u \mathbf{v}_u + E_v \mathbf{v}_v. \quad (3)$$

The array output signal covariance matrix is

$$\mathbf{R}_s = \langle \mathbf{v}_s \mathbf{v}_s^H \rangle = \mathbf{V} \mathbf{\Sigma} \mathbf{V}^H, \quad (4)$$

where we have introduced $\mathbf{V} = [\mathbf{v}_u, \mathbf{v}_v]$. Assuming that the phased array system noise can be characterized by a noise covariance matrix \mathbf{R}_n , the covariance matrix of the array output voltage \mathbf{v} can be described as

$$\mathbf{R} = \langle \mathbf{v} \mathbf{v}^H \rangle = \mathbf{R}_s + \mathbf{R}_n = \mathbf{V} \mathbf{\Sigma} \mathbf{V}^H + \mathbf{R}_n. \quad (5)$$

The noise covariance matrix can be determined using an off-source measurement on an empty part of the sky, i.e., a part of the sky without significant source structure. The noise covariance matrix includes factors such as noise coupling and spillover noise.

The beamformer output covariance matrix is obtained from the beamformer output voltages, $v_1 = \mathbf{w}_1^H \mathbf{v}$ and $v_2 = \mathbf{w}_2^H \mathbf{v}$, by

$$\mathbf{R}_o = \left\langle \begin{bmatrix} v_1 \\ v_2 \end{bmatrix} \begin{bmatrix} v_1 \\ v_2 \end{bmatrix}^H \right\rangle = \begin{bmatrix} \langle |v_1|^2 \rangle & \langle v_1 v_2^* \rangle \\ \langle v_1^* v_2 \rangle & \langle |v_2|^2 \rangle \end{bmatrix}. \quad (6)$$

In terms of the signal and noise covariance matrices introduced earlier, this can be written as

$$\begin{aligned} \mathbf{R}_o &= \begin{bmatrix} \mathbf{w}_1^H \mathbf{R} \mathbf{w}_1 & \mathbf{w}_1^H \mathbf{R} \mathbf{w}_2 \\ \mathbf{w}_2^H \mathbf{R} \mathbf{w}_1 & \mathbf{w}_2^H \mathbf{R} \mathbf{w}_2 \end{bmatrix} \\ &= \begin{bmatrix} \mathbf{w}_1 & \mathbf{w}_2 \end{bmatrix}^H \mathbf{R} \begin{bmatrix} \mathbf{w}_1 & \mathbf{w}_2 \end{bmatrix} \\ &= \mathbf{W}^H (\mathbf{V} \mathbf{\Sigma} \mathbf{V}^H + \mathbf{R}_n) \mathbf{W} \\ &= \mathbf{R}_{o,s} + \mathbf{R}_{o,n}, \end{aligned} \quad (7)$$

where $\mathbf{R}_{o,s}$ and $\mathbf{R}_{o,n}$ are the beamformer output covariance matrices due to the signal and the noise, respectively.

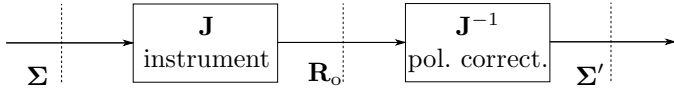


Fig. 2. A system level view of a radio polarimeter.

B. Useful concepts

1) *Sensitivity equivalence*: The combined sensitivity, expressed as the ratio of effective aperture area A_e and system temperature T_{sys} , of the two beamformer outputs, the beam pair sensitivity, is determined by a linear combination of the two output signals. This can be obtained from [8]

$$\frac{A_e}{T_{\text{sys}}} = \frac{k_b B}{S_{\text{sig}}} \text{SNR} = \frac{k_b B}{S_{\text{sig}}} \frac{\mathbf{a}^H \mathbf{W}^H \mathbf{R}_s \mathbf{W} \mathbf{a}}{\mathbf{a}^H \mathbf{W}^H \mathbf{R}_n \mathbf{W} \mathbf{a}}, \quad (8)$$

where $\mathbf{a} = [a_1, a_2]^T$ is an arbitrary vector other than the null vector, S_{sig} is the power flux density of the received signal expressed in W/m^2 , k_b is the Boltzmann constant and B is the bandwidth.

As shown in [9], the beam pair sensitivity is bounded by

$$\frac{k_b B}{S_{\text{sig}}} \lambda_{\min} \leq \frac{A_e}{T_{\text{sys}}} \leq \frac{k_b B}{S_{\text{sig}}} \lambda_{\max}, \quad (9)$$

where λ_{\min} and λ_{\max} are the smallest and largest eigenvalue of

$$\mathbf{C} = \mathbf{V}^H \mathbf{W} (\mathbf{W}^H \mathbf{R}_n \mathbf{W})^{-1} \mathbf{W}^H \mathbf{V}. \quad (10)$$

By replacing \mathbf{W} with $\mathbf{W}' = \mathbf{W}\mathbf{A}$ where \mathbf{A} is an arbitrary invertible 2×2 matrix, it is easily seen that \mathbf{C} is independent of a linear transformation of the beam subspace and therefore of the polarimetric calibration. We will refer to beam pairs that are related by such a transformation as sensitivity equivalent beam pairs. This transformation signifies that all sensitivity equivalent beam pairs lie within the same two dimensional subspace of the N -dimensional space of complex valued N -element vectors. There are many possible rank two subspaces, but only one that includes the maximum sensitivity beamformer. Within each two dimensional subspace, there is one unique beam pair that is polarimetrically calibrated.

Transformations applied after beamforming necessarily stay within one two dimensional subspace. Sensitivity equivalence implies that the beamformer weights can be described as $\mathbf{W}\mathbf{J}_{\text{cor}}$, where \mathbf{J}_{cor} is a 2×2 matrix describing a polarimetric correction. If a beamformer can be formulated in this form, the polarimetric correction can be done after beamforming without affecting the sensitivity bounds of the beamformer given by (9).

2) *Jones matrices*: In the noise free case or with noise estimated and subtracted, (7) reduces to

$$\mathbf{R}_o = \mathbf{W}^H \mathbf{V} \Sigma \mathbf{V}^H \mathbf{W} = \mathbf{J} \Sigma \mathbf{J}^H, \quad (11)$$

where we have introduced the 2×2 Jones matrix $\mathbf{J} = \mathbf{W}^H \mathbf{V}$. This Jones matrix represents the transfer function of the instrument including antennas, receiver chains and beamforming scheme, that transforms the two input voltages adhering to a suitable polarimetric definition into two output voltages, possibly adhering to another polarimetric definition. Figure 2

provides a system level view of the phased array antenna system. The polarimetric properties of the source are defined by the source covariance matrix Σ . This is transformed to the beamformer output covariance matrix \mathbf{R}_o (equal to $\mathbf{R}_{o,s}$ in the noise free case), that is used for further processing to produce a reconstructed source covariance matrix Σ' that should ideally be proportional to Σ . An ideal system does not require polarimetric correction, since it has $\mathbf{J} = \mathbf{I}$, where \mathbf{I} denotes the identity matrix, i.e., it leaves the covariance matrix of the input signal unchanged and does not introduce so-called instrumental polarization. Since $\mathbf{J} = \mathbf{W}^H \mathbf{V}$, the instrumental polarization introduced by the antennas and other analog electronics can be compensated for in the beamformer.

3) *Max-SNR beamforming*: The highest signal-to-noise ratio (SNR) for the u - and v -polarized signal is achieved by the max-SNR beamformer [12]

$$\mathbf{W}_{\text{SNR}} = \mathbf{R}_n^{-1} \mathbf{V}. \quad (12)$$

Although this beamformer does not calibrate the polarimetric response of the array, it does provide the maximum sensitivity.

4) *Optimal beamforming*: If we know the voltage response vectors to two perfectly orthogonally polarized signals, \mathbf{v}_u and \mathbf{v}_v , and the noise covariance matrix, \mathbf{R}_n , we can derive optimal weights for the beamformer that ensures minimization of the noise in the measurement and perfect reconstruction of the polarization properties of the source. This optimization can be formulated as the constrained minimization problem

$$\mathbf{W}_{\text{opt}} = \underset{\mathbf{W}}{\text{argmin}} \text{tr} (\mathbf{W}^H \mathbf{R}_n \mathbf{W}) \quad \text{subject to} \quad \mathbf{W}^H \mathbf{V} = \mathbf{I}. \quad (13)$$

It can be shown that the solution to this optimization problem is given by [9]

$$\mathbf{W}_{\text{opt}} = \mathbf{R}_n^{-1} \mathbf{V} (\mathbf{V}^H \mathbf{R}_n^{-1} \mathbf{V})^{-1}. \quad (14)$$

This pair of beamformer weight vectors minimizes the response to the system noise while constrained to be polarimetrically calibrated. We will refer to this calibration method as the optimal method. The factor $(\mathbf{V}^H \mathbf{R}_n^{-1} \mathbf{V})^{-1}$ can be interpreted as a Jones matrix that applies a polarimetric correction to the max-SNR beamformer weights. If the Jones matrix is invertible, an assumption that should hold for polarimetric arrays, the optimal beamformer is sensitivity equivalent to the max-SNR beamformer. Hence, the optimal and the max-SNR beamformer weights span the same subspace and within this subspace, the optimal beamformer picks the weight vectors that provide the optimal polarimetric response. The same response can be achieved with the max-SNR beamformer only with an additional polarimetric correction after beamforming.

5) *XPD and XPI*: Following standard IEEE definitions, the cross-polarization discrimination (XPD) and cross-polarization isolation (XPI) can be expressed in terms of Jones matrix elements as [13]

$$\text{XPD}_u = \frac{|J_{11}|^2}{|J_{21}|^2} \quad \text{XPD}_v = \frac{|J_{22}|^2}{|J_{12}|^2} \quad (15a)$$

$$\text{XPI}_u = \frac{|J_{11}|^2}{|J_{12}|^2} \quad \text{XPI}_v = \frac{|J_{22}|^2}{|J_{21}|^2}. \quad (15b)$$

6) *Intrinsic cross-polarization ratio*: Since the goal of polarimetric phased arrays is to reconstruct the polarimetric properties of the source signal, preservation of these polarimetric properties by the Jones matrix \mathbf{J} of the instrument need not be a design goal by itself as long as the source coherency can be reconstructed by a polarimetric correction \mathbf{J}^{-1} . This idea led to the definition of the intrinsic cross-polarization ratio (IXR). The IXR provides a measure for the reconstructability of Σ (invertibility of \mathbf{J}) and is defined as [13]

$$\text{IXR} = \left(\frac{\kappa(\mathbf{J}) + 1}{\kappa(\mathbf{J}) - 1} \right)^2, \quad (16)$$

where $\kappa(\mathbf{J})$ denotes the condition number of \mathbf{J} .

The IXR provides an upper limit on the relative error in the reconstructed Stokes vector \mathbf{S} that is given by [13]

$$\frac{\|\Delta\mathbf{S}_s\|}{\|\mathbf{S}_s\|} \lesssim \left(1 + \frac{4\sqrt{\text{IXR}}}{1 + \text{IXR}} + \dots \right) \left(\frac{\|\Delta\mathbf{M}\|}{\|\mathbf{M}\|} + \frac{\|\Delta\mathbf{S}_{o,s}\|}{\|\mathbf{S}_{o,s}\|} \right), \quad (17)$$

where $\|\cdot\|$ denotes the Euclidian norm, $\|\Delta\mathbf{M}\|$ denotes the calibration error in the Mueller matrix and $\|\Delta\mathbf{S}\|$ denotes the measurement error in the Stokes vector. Note that the term involving the IXR describes an increase of the relative Stokes error compared to a system with perfectly orthogonally polarized feeds. For example, if the noise on the observation causes a relative error (uncertainty) on the measured Stokes vector of 1% and the relative error in the instrument model (due to, e.g., calibration errors) is 1% as well, such a system would have about 1.4% relative error in the reconstructed Stokes vector. An IXR of 25 dB may (note that (17) gives an upper bound) cause a 22% increase in this error, which may therefore increase to 1.7%.

III. CALIBRATION USING AN UNPOLARIZED SOURCE

The majority of continuum extragalactic sources, which are typically used for calibration, are weakly polarized or unpolarized. Calibration of radio telescopes therefore requires methods that exploit unpolarized reference sources. In this section, we discuss three proposed methods. We will see that we cannot do a full polarimetric calibration of the system only using an unpolarized source. Two of the proposed methods rely on the intrinsic polarimetric characteristics of the instrument.

A. Eigenvector method

For a polarimetric array, neglecting estimation error, the signal covariance matrix \mathbf{R}_s measured on an unpolarized source has rank 2. If the system consists of two sets of orthogonally polarized feeds, there is hardly any correlation between the receiving elements in the two sets when measuring an unpolarized source. Intuitively, the two dominant eigenvectors will each be associated with one set of feeds. This naturally suggests the use of the two principal eigenvectors, \mathbf{v}_1 and \mathbf{v}_2 , to form the maximum SNR eigenvector beamformer weight vectors [10]

$$\mathbf{W}_{\text{eig}} = \mathbf{R}_n^{-1} \mathbf{V}_{\text{eig}}, \quad (18)$$

where $\mathbf{V}_{\text{eig}} = [\mathbf{v}_1, \mathbf{v}_2]$. We will refer to this approach as the eigenvector method.

To compare this beamformer with the optimal solution presented in the previous section, we note that the voltage response vectors \mathbf{v}_u and \mathbf{v}_v must span the same subspace as the eigenvectors \mathbf{v}_1 and \mathbf{v}_2 . This implies that

$$\mathbf{V} = \mathbf{V}_{\text{eig}} \mathbf{J}_{\text{eig}}, \quad (19)$$

where the 2×2 Jones matrix \mathbf{J}_{eig} describes the transformation from \mathbf{v}_1 and \mathbf{v}_2 to \mathbf{v}_u and \mathbf{v}_v . The weights obtained by the eigenvector method can thus be described as

$$\mathbf{W}_{\text{eig}} = \mathbf{R}_n^{-1} \mathbf{V} \mathbf{J}_{\text{eig}}^{-1}, \quad (20)$$

Substitution in (14) gives

$$\begin{aligned} \mathbf{W}_{\text{opt}} &= \mathbf{R}_n^{-1} \mathbf{V}_{\text{eig}} \mathbf{J}_{\text{eig}} (\mathbf{V}^H \mathbf{R}_n^{-1} \mathbf{V}_{\text{eig}} \mathbf{J}_{\text{eig}})^{-1} \\ &= \mathbf{W}_{\text{eig}} (\mathbf{V}^H \mathbf{W}_{\text{eig}})^{-1} \end{aligned} \quad (21)$$

This shows that the two beamformers are sensitivity equivalent. This implies that one beamformer can be transformed into the other by an additional polarimetric correction after beamforming.

Unfortunately, a single measurement on an unpolarized source does not provide sufficient information for full polarimetric calibration. This can be demonstrated by substitution of (19) in (4) with $\Sigma = \mathbf{I}$. This gives

$$\mathbf{R}_s = \mathbf{V} \mathbf{V}^H = \mathbf{V}_{\text{eig}} \mathbf{J}_{\text{eig}} \mathbf{J}_{\text{eig}}^H \mathbf{V}_{\text{eig}}^H, \quad (22)$$

If we replace \mathbf{J}_{eig} by $\mathbf{J}'_{\text{eig}} = \mathbf{J}_{\text{eig}} \mathbf{U}$, where \mathbf{U} is an arbitrary unitary matrix, we get

$$\begin{aligned} \mathbf{R}_s &= \mathbf{V}_{\text{eig}} \mathbf{J}'_{\text{eig}} \mathbf{J}'_{\text{eig}}{}^H \mathbf{V}_{\text{eig}}^H \\ &= \mathbf{V}_{\text{eig}} \mathbf{J}_{\text{eig}} \mathbf{U} \mathbf{U}^H \mathbf{J}_{\text{eig}}^H \mathbf{V}_{\text{eig}}^H \\ &= \mathbf{V}_{\text{eig}} \mathbf{J}_{\text{eig}} \mathbf{J}_{\text{eig}}^H \mathbf{V}_{\text{eig}}^H, \end{aligned} \quad (23)$$

i.e., we get exactly the same solution. This shows that our measurement cannot discriminate between \mathbf{J}_{eig} and \mathbf{J}'_{eig} , which implies that the relation between \mathbf{V} and \mathbf{V}_{eig} given by (19) has a unitary ambiguity.

This polarimetric calibration problem has been studied in detail by Hamaker [14]. He found that the physical significance of the aforementioned unitary ambiguity is described by polconversion and polrotation. Polconversion is the effect that part of the unpolarized power is detected as (“converted to”) polarized power. Polrotation refers to a rotation or axial ratio change of the polarization ellips. This unitary ambiguity can be resolved by additional measurements on two distinctly polarized sources or by imposing additional constraints on the instrumental Jones matrix as discussed in [14], [15]. Relying on the intrinsic polarimetric purity of the receiving elements as discussed in the next sections is an example of such an additional constraint. In Sec. IV, we demonstrate the impact of ignoring this ambiguity using a simple dipole model.

B. Eigenvector method with bi-scalar approximate calibration

Since the eigenvector method produces a pair of beamformer output signals that are only polarimetrically correct up to a unitary matrix, we would like to find a correction to ensure well-defined polarimetric characteristics at the beamformer output. This can be achieved by assuming that the

system consists of two sets of feeds that have an orthogonal polarimetric response as proposed in [9]. For analysis of such a system, it is convenient to partition the signal covariance matrix as

$$\mathbf{R}_s = \begin{bmatrix} \mathbf{R}_{s,uu} & \mathbf{R}_{s,uv} \\ \mathbf{R}_{s,vu} & \mathbf{R}_{s,vv} \end{bmatrix}. \quad (24)$$

The submatrices are $N/2 \times N/2$ matrices and we have assumed that the first $N/2$ elements are optimally matched to u -polarized signals while the second $N/2$ elements are optimally matched to v -polarized signals. The matrices

$$\mathbf{R}_{s,u} = \begin{bmatrix} \mathbf{R}_{s,uu} & \mathbf{0} \\ \mathbf{0} & \mathbf{0} \end{bmatrix} \quad \text{and} \quad \mathbf{R}_{s,v} = \begin{bmatrix} \mathbf{0} & \mathbf{0} \\ \mathbf{0} & \mathbf{R}_{s,vv} \end{bmatrix}, \quad (25)$$

have rank one with principal eigenvectors $\tilde{\mathbf{v}}_u$ and $\tilde{\mathbf{v}}_v$ respectively. These vectors can be used to find the approximate Jones matrix

$$\tilde{\mathbf{J}} = \mathbf{W}_{\text{eig}}^H \tilde{\mathbf{V}}, \quad (26)$$

where $\tilde{\mathbf{V}} = [\tilde{\mathbf{v}}_u, \tilde{\mathbf{v}}_v]$. This Jones matrix can be used to calibrate the beam pair to obtain

$$\mathbf{W}_{\text{approx}} = \mathbf{W}_{\text{eig}} \tilde{\mathbf{J}}^{-H}. \quad (27)$$

Since $\tilde{\mathbf{v}}_u$ and $\tilde{\mathbf{v}}_v$ are only determined up to a scale factor, further normalization may be required as discussed in [9].

C. Bi-scalar method

Most astronomical phased array systems consist of two sets of feeds, each optimally matched to a single polarization. This can be exploited by calibrating and beamforming both feed sets separately, which simplifies the design of the system considerably, since this approach requires two identical processing systems that each have to deal with only $N/2$ signals, instead of a single system with N inputs, thereby simplifying signal routing and saving half the compute power for correlation of the input signals. This is referred to as a bi-scalar approach. Since this method treats both sets separately, it ignores the cross-terms between the two sets of elements in the signal and noise covariance matrices. For our analysis, it is therefore convenient to partition these matrices as indicated in (24). We can then formulate the bi-scalar beamformer as

$$\mathbf{W}_{\text{bi-s}} = \begin{bmatrix} \mathbf{R}_{n,uu}^{-1} & \mathbf{0} \\ \mathbf{0} & \mathbf{R}_{n,vv}^{-1} \end{bmatrix} [\tilde{\mathbf{v}}_u, \tilde{\mathbf{v}}_v]. \quad (28)$$

If the two feed sets are perfectly matched to u - and v -polarized signals respectively such that $\mathbf{R}_{s,uv} = \mathbf{R}_{s,vu} = \mathbf{0}$, the bi-scalar approach gives the same result as the optimal method or the eigenvector method and is therefore sensitivity equivalent. Otherwise, the bi-scalar beamformer introduces a beamforming error due to neglecting the cross-polarization response of the elements. The impact on sensitivity depends on the antenna responses. Using (9) we can determine the loss in sensitivity for a specific antenna system.

A full polarimetric beamformer combines the u -polarized power picked up as co-polarization in the u -elements and as cross-polarization of the v -elements. The latter contribution is ignored by a bi-scalar beamformer. To get a feel for the

implications of ignoring this term, we note that, in general, the voltage output of the beamformer is given by

$$\begin{aligned} \mathbf{W}^H \mathbf{v} &= \begin{bmatrix} \mathbf{w}_{u,u}^H & \mathbf{w}_{u,v}^H \\ \mathbf{w}_{v,u}^H & \mathbf{w}_{v,v}^H \end{bmatrix} \mathbf{v} \\ &= \left(\begin{bmatrix} \mathbf{w}_{u,u}^H & \mathbf{0} \\ \mathbf{0} & \mathbf{w}_{v,v}^H \end{bmatrix} + \begin{bmatrix} \mathbf{0} & \mathbf{w}_{u,v}^H \\ \mathbf{w}_{v,u}^H & \mathbf{0} \end{bmatrix} \right) \mathbf{v}, \end{aligned} \quad (29)$$

where $\mathbf{w}_{u,v}$ denotes the weight vector assigned to the u -polarized elements for the beamformer output associated with v -polarized signals and similar definitions for $\mathbf{w}_{u,u}$, $\mathbf{w}_{v,u}$ and $\mathbf{w}_{v,v}$.

Since the weights $\mathbf{w}_{u,v}$ need to be applied to the u -polarized elements although they are associated with v -polarized signals, we can exploit the ability of typical PAF systems to form a cross-polarization beam for the signals from the u -polarized elements and similarly for the v -polarized elements [16]. Once both co- and cross-polarized beams are formed, we can add the appropriate beam signals to reconstruct the output signals of a full polarimetric beamformer. This approach doubles the number of beams to be formed. Since the total bandwidth of the beamformer (number of beams times the bandwidth per beam) is limited by the digital hardware, we can only apply this scheme by sacrificing half the bandwidth per beam to allow for twice as many beams (the co- and cross-polarized beams). This reduces the sensitivity for continuum sources by a factor $\sqrt{2}$ and the survey speed by a factor 2. This may not seem attractive, but some observations, such as interferometric observations with other telescope systems, may not need the full bandwidth of the system in which case this scheme may be applied without its drawbacks. This is an important conclusion for instruments with a bi-scalar design that can form multiple beams within the FoV like APERTIF. However, calculation of these weights requires knowledge of the full signal and noise covariance matrices, which implies that these systems still need to provide a facility that can correlate the signals from any feed pair in the system for calibration of the array, although, for example, with a reduced bandwidth.

IV. DIPOLE MODEL ANALYSIS

In this section, we present a simple dipole model and use it to provide some insight in the impact of the unitary ambiguity discussed in the previous section on the polarimetric performance of the instrument. We also use this dipole model to assess the impact of non-orthogonality in the polarimetric response of the receiving elements for the methods that rely on the intrinsic orthogonality of the feed sets.

A. Description of the dipole model

For this simple model, we assume that each antenna consists of two co-located ideal dipoles in the (x, y) -plane making an angle ϕ with each other. The open circuit responses of the dipoles for broadside incidence are then proportional to

$$\mathbf{V}_{\text{oc}} \propto \begin{bmatrix} 1 & 0 \\ \gamma \cos \phi & \gamma \sin \phi \end{bmatrix}, \quad (30)$$

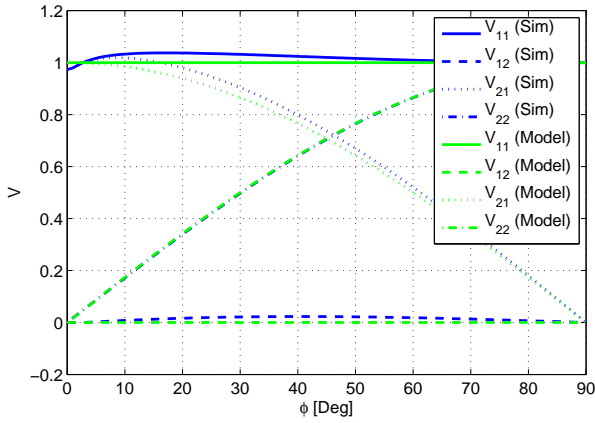


Fig. 3. Comparison between the elements of \mathbf{V}_{oc} predicted by an EM-simulation [17] of two crossed short dipoles and those given by (30) assuming $\gamma = 1$. The curve for the modeled V_{22} overlaps with the simulated V_{22} .

where γ is the gain of the second dipole assuming that the receive voltage of the first dipole is 1 V. The open circuit signal covariance matrix for an unpolarized source is then proportional to

$$\mathbf{R}_{s,oc} = \mathbf{V}_{oc} \mathbf{V}_{oc}^H \propto \begin{bmatrix} 1 & \gamma \cos \phi \\ \gamma \cos \phi & \gamma^2 \end{bmatrix}. \quad (31)$$

Using $\mathbf{R}_{n,oc} = 8kT \text{Re}\{\mathbf{Z}_A\}$, where \mathbf{Z}_A denotes the antenna impedance matrix, we find that, to first order,

$$\mathbf{R}_{n,oc} \propto 8kT R_{rad} \begin{bmatrix} 1 & \gamma \cos \phi \\ \gamma \cos \phi & \gamma^2 \end{bmatrix}, \quad (32)$$

where R_{rad} is the radiation resistance. In the loaded case, we have $\mathbf{R}_s = \mathbf{Q} \mathbf{R}_{s,oc} \mathbf{Q}^H$ and $\mathbf{R}_n = \mathbf{Q} \mathbf{R}_{n,oc} \mathbf{Q}^H$, where $\mathbf{Q} = \mathbf{Z}_R (\mathbf{Z}_R + \mathbf{Z}_A)^{-1}$ with \mathbf{Z}_R denoting the input impedance of the receiving network. We need expressions for the imaginary part of the antenna impedance matrix and \mathbf{Z}_R to obtain expressions for \mathbf{R}_s and \mathbf{R}_n , which will be more tedious than the expressions for their open circuited counterparts given above. For our educational example, we therefore choose to use the open circuited case, i.e., to assume that the antenna ports are connected to voltage amplifiers.

To verify this seemingly simple model, we did an EM-simulation [17] with two crossed short dipoles making an angle ϕ with length $L = \lambda/4$, width $w = \lambda/640$ and inter-element distance $\Delta z = 2w$. Figure 3 compares the open circuit voltages obtained from the EM-simulation with those described by the analytical model while Fig. 4 makes a similar comparison for the elements of the noise covariance matrix. For convenience, we have assumed $8kT R_{rad} = 1$ and $\gamma = 1$. These results show that our analytical model is rather accurate, especially for the crucial range where ϕ is close to 90° . The differences are primarily due to the finite strip width of the numerical model.

B. Eigenvalue decomposition

For the analysis of the eigenvector method, we compute the eigenvectors of the signal covariance matrix given by (31). Since we are interested in the impact of non-orthogonality

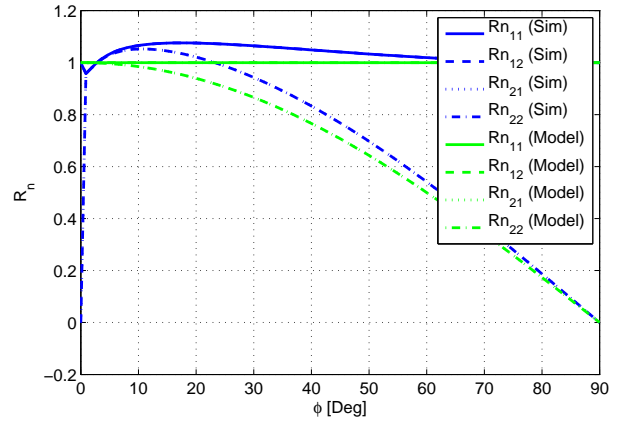


Fig. 4. Comparison between the elements of $\mathbf{R}_{n,oc}$ predicted by the EM-simulation [17] of two crossed short dipoles and those given by (32) assuming $\gamma = 1$ and $8kT R_{rad} = 1$. The results for the two off-axis elements and the two on-axis elements of $\mathbf{R}_{n,oc}$ are identical, as expected from symmetry.

between the dipoles, we assume that the dipoles have the same gain, i.e., that $\gamma = 1$. Solving for the eigenvalues using the characteristic polynomial, we find that

$$\lambda_{1,2} = 1 \pm \cos \phi. \quad (33)$$

We can now solve for the eigenvectors associated with each eigenvalue. It is straightforward to show that for $\phi \neq \pi/2 \pmod{\pi}$,

$$\mathbf{V}_{eig} = \frac{1}{2} \sqrt{2} \begin{bmatrix} 1 & 1 \\ 1 & -1 \end{bmatrix} \quad (34)$$

and that $\mathbf{V}_{eig} = \mathbf{I}$ if $\phi = \pi/2 \pmod{\pi}$. Although \mathbf{V}_{eig} shows a discontinuity at $\phi = \pi/2$, we will see that the response of the system remains continuous when using the eigenvector method. Although this analysis was done for a single antenna consisting of two crossed dipoles, it can easily be shown that the results also hold for an array of identical antennas where the coupling between antenna pairs is negligible. This implies that the results obtained from the analysis of a single antenna can also be applied to a full array.

C. Impact of the unitary ambiguity

In this section we will demonstrate the effect of the unitary ambiguity by comparing the Jones matrix and beamformer output signal covariance matrix for the optimal method and the eigenvector method. It is straightforward to show that for the optimal method

$$\mathbf{J}_{opt} = \mathbf{W}_{opt}^H \mathbf{V} = \mathbf{I} \quad (35)$$

such that

$$\mathbf{R}_{o,s} = \mathbf{J}_{opt} \mathbf{J}_{opt}^H = \mathbf{I}. \quad (36)$$

In a similar way, we can show that for the eigenvector method

$$\mathbf{J}_{eig} = \mathbf{W}_{eig}^H \mathbf{V} = \frac{1}{\sqrt{2}} \begin{bmatrix} 1 & \frac{1-\cos \phi}{\sin \phi} \\ 1 & -\frac{1+\cos \phi}{\sin \phi} \end{bmatrix}, \quad (37)$$

where we assumed a proportionality constant in (32) equal to unity. It is interesting to note that substituting $\phi = \pi/2$

in (37) gives the same result as obtained for $\mathbf{V}_{\text{eig}} = \mathbf{I}$, i.e., the discontinuity at $\phi = \pi/2 \bmod \pi$ found in the eigenvalue decomposition vanishes when the result is applied in the eigenvector beamforming scheme. Using (37) we find that the beamformer output signal covariance matrix for the eigenvector method is given by

$$\mathbf{R}_{\text{o,s}} = \begin{bmatrix} 2 \sin^2(\phi/2) & 0 \\ 0 & 2 \cos^2(\phi/2) \end{bmatrix}. \quad (38)$$

Equation (37) shows that if ϕ is close to 90° , i.e., if the polarimetric responses of the dipoles are (almost) orthogonal, the magnitudes of the entries of the Jones matrix are (almost) equal. This indicates that the two input polarizations aligned with \hat{u} and \hat{v} are mixed to form two output signals that are aligned with two other axes. However, if we look at the beamformer output signal covariance matrix for an unpolarized source, it seems that the system preserves the properties of the source. This counter intuitive result can be explained by the unitary ambiguity, which works on the Jones matrix, but cancels itself in the beamformer output signal covariance matrix, i.e., we have developed a beamforming scheme that gives perfect results for unpolarized sources, but gives erroneous results in observations on polarized sources.

It will also yield wrong results if the two beamformer output signals are correlated to the two beamformer output signals of another antenna system with a well-defined polarization. This situation may occur in practice when multiple telescope systems are linked together. Hence, it is important that the voltage response of the system described by the Jones matrix is well defined. This argument shows that the eigenvector method is not suitable for use in an actual system unless appropriate corrections are made to the beamformer output signals.

If we apply the bi-scalar approximate calibration discussed in Sec. III-B to the dipole model, we find

$$\mathbf{J}_{\text{approx}} = \mathbf{W}_{\text{approx}}^H \mathbf{V} = \begin{bmatrix} 1 & 0 \\ \frac{\cos \phi}{\sin \phi} & 1 \end{bmatrix}. \quad (39)$$

This shows that if the dipoles are close to orthogonal, i.e., if $\phi \approx 90^\circ$, then $\mathbf{J}_{\text{approx}} \approx \mathbf{I}$, which is close to the desired response. This shows that the unitary ambiguity can be resolved by the intrinsic properties of the system, but that the accuracy of that correction depends on the orthogonality in the polarimetric response of the two feeds.

D. Impact of non-orthogonality

In our next simulation, we look at the impact of non-orthogonality between the dipoles by comparing the IXR as defined in (16) of the beamformers for different inter-dipole angles. Since $\mathbf{J} \propto \mathbf{I}$ for the optimal method, the IXR is infinite for this method regardless of the orientation of the dipoles. The IXR for the optimal method is therefore not shown in Fig. 5. As derived in the appendix, the IXR for the eigenvector method is conveniently described by

$$\text{IXR}_{\text{eig}} = \left(\frac{1 + \tan(\phi/2)}{1 - \tan(\phi/2)} \right)^2. \quad (40)$$

Comparison of the IXR for the bi-scalar method and for the eigenvector method with and without bi-scalar approximate

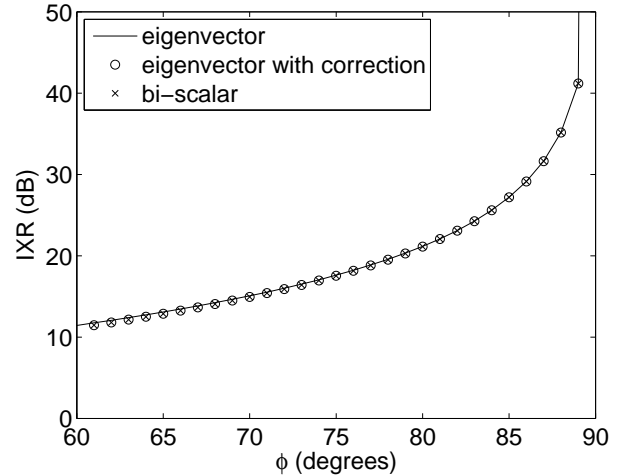


Fig. 5. IXR as function of the angle between the two dipoles for the eigenvector method, the eigenvector method with bi-scalar correction and the bi-scalar beamformer.

calibration shows that the eigenvector methods are not able to produce a pair of beamformer output signals that is more suitable for reconstruction of the polarimetric properties of the input signal than the bi-scalar beamformer when the dipoles are close to orthogonal. This indicates, that these methods rely on the polarimetric quality of the antenna system. An intuitive explanation for this result, is that all these methods use an unpolarized source for system calibration and thus have to rely on the intrinsic polarization quality of the antenna system to resolve the unitary ambiguity. Since most astronomical calibration sources are not or only weakly polarized, this implies that a well-designed antenna system is invaluable, even given the material presented in this paper. An IXR of 25 dB limits the potential increase in the relative Stokes error during reconstruction to 22% as indicated by (17), which requires $\phi \geq 83.7^\circ$.

Since the eigenvector method with bi-scalar correction is sensitivity equivalent to the optimal beamformer and has the same IXR as the bi-scalar beamformer, which has lower sensitivity than the optimal method, it seems to be the best method for calibration of a practical radio telescope system on one of the available celestial calibration sources, which are usually unpolarized.

It follows from (39) and the definitions given by (15a) and (15b), that for the eigenvector method with bi-scalar correction

$$\begin{aligned} \text{XPD}_{\text{u}} &= \tan^2 \phi & \text{XPD}_{\text{v}} &= \infty \\ \text{XPI}_{\text{u}} &= \infty & \text{XPI}_{\text{v}} &= \tan^2 \phi. \end{aligned}$$

Similarly, we find for the bi-scalar beamformer that

$$\begin{aligned} \text{XPD}_{\text{u}} &= \frac{1}{\cos^2 \phi \sin^2 \phi} & \text{XPD}_{\text{v}} &= \infty \forall \phi \neq 0 \\ \text{XPI}_{\text{u}} &= \infty & \text{XPI}_{\text{v}} &= \tan^2 \phi. \end{aligned}$$

These results are asymmetric in the two polarizations, since we defined our dipole model such that one dipole is aligned with one of the polarization axes. Since rotation of the polarization axes is described by a unitary matrix, such a rotation does

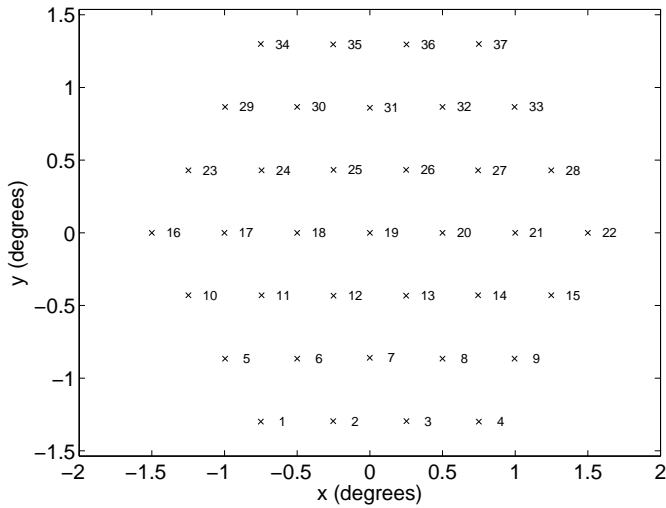


Fig. 6. Arrangement of the 37 beams produced by the APERTIF system over the FoV of the WSRT.

not affect the condition number of the Jones matrix making the IXR insensitive to such a transformation. These results indicate that $\phi \geq 83.7^\circ$, required to achieve an IXR of 25 dB, corresponds to an XPD of at least 19 dB.

V. BI-SCALAR BEAMFORMER PERFORMANCE

The bi-scalar approach is commonly applied in actual phased array systems. However, in this paper, we have shown that the bi-scalar beamformer is not sensitivity equivalent to the optimal beamformer and that it relies on the intrinsic polarimetric orthogonality of the feed system. We would therefore like to assess the sensitivity and polarimetric performance of the bi-scalar beamformer in an actual system to see whether it provides acceptable performance. For this assessment, we use results from EM-simulations from the Aperture Tile-in-Focus (APERTIF) project. The goal of this project is to develop and build a PAF system for the Westerbork Synthesis Radio Telescope (WSRT) located in The Netherlands to increase its field-of-view (FoV) [5]. The APERTIF system will be able to produce 37 beams on the sky that will probably be arranged in a hexagonal pattern separated by about half power beam width as indicated in Fig. 6.

A. Performance in the compound beam centers

The APERTIF system was simulated using a full-wave EM package [18]. Figure 7 shows the average sensitivity of the two beamformer outputs for the optimal beamformer and the bi-scalar beamformer, while Fig. 8 shows the IXR of the bi-scalar beamformer. All results were obtained for the beam centers at 1.4 GHz. From these results, we conclude that use of a bi-scalar beamformer leads to about 4.5% sensitivity loss compared to the optimal beamformer and that the typical IXR will be about 38 dB with a peak value of 59 dB for the central compound beam. Note that the IXR in Fig. 8 is asymmetric with respect to the central beam with index 19. This is caused by the asymmetrical circular cavity terminating the tapered slot which has been bended sideways to reduce the length

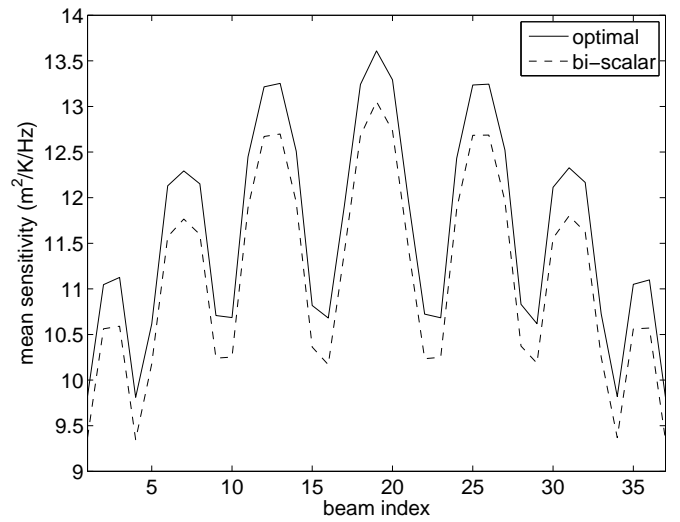


Fig. 7. Average sensitivity of the two beamformer output signals for the bi-scalar method and the optimal beamformer at the centers of the 37 beams formed by the APERTIF system. The beam indices correspond to the beam numbers given in Fig. 6.

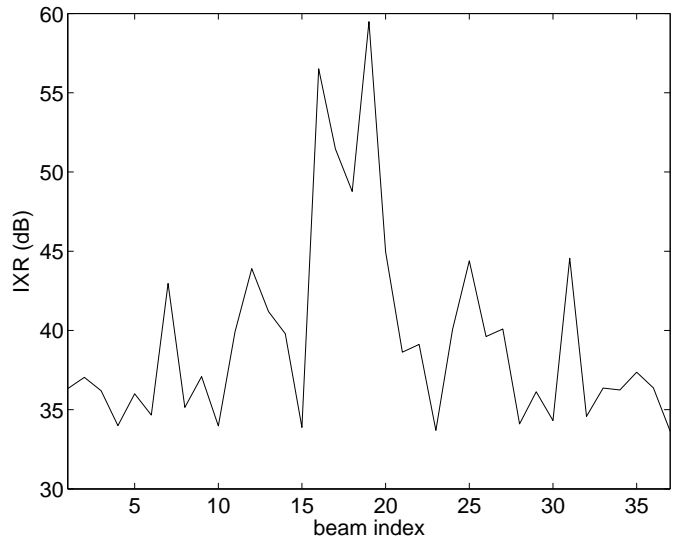


Fig. 8. IXR of the bi-scalar beamformer at the centers of the 37 APERTIF beams. The beam numbers correspond to the beam numbering shown in Fig. 6.

of the microstrip transmission line feeding the slot. Also, the antenna elements are positioned diagonally over a square ground plane which results in different element configurations per polarization at the corners of the array.

These results are similar to those found for an earlier APERTIF prototype system [16], [18]. Measurements done with the APERTIF prototype system mounted on one of the WSRT dishes confirmed the sensitivity loss, but also indicated that the practicalities of an actual system reduce the ratio of cross- to co-polarized power observed on an unpolarized source to about 28 dB [16]. This was considered acceptable, because the cross-polarization level can be improved by applying appropriate polarimetric corrections to the beamformer output signals while the sensitivity loss can be recovered by

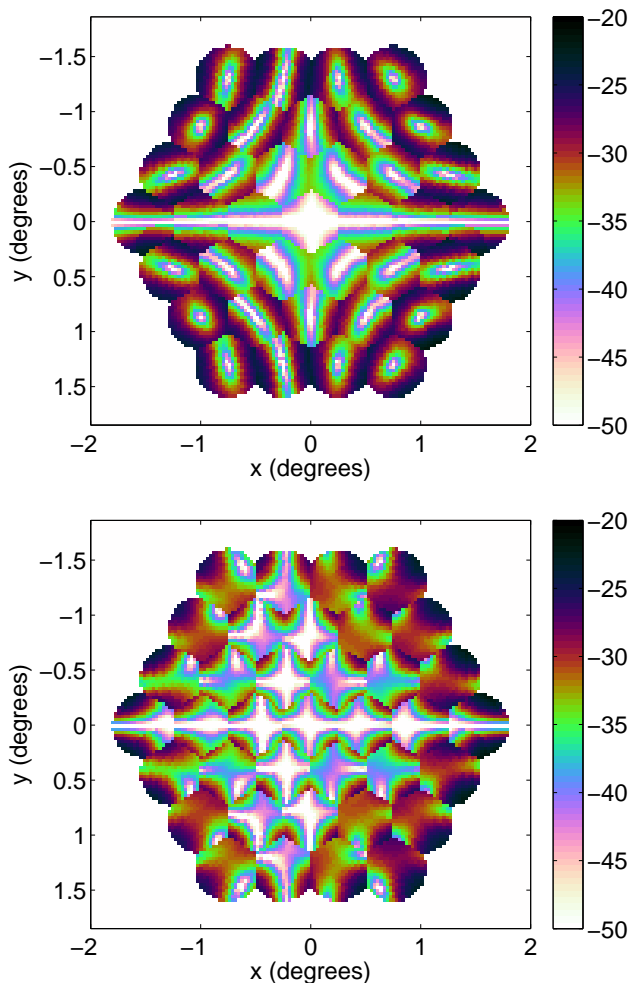


Fig. 9. $|J_{12}|$ for all 37 beams produced by the APERTIF system for the optimal beamformer (top) and bi-scalar beamformer (bottom). The color scale has units of dB with respect to the value of $|J_{11}|$ at the peak of the central compound beam.

forming cross- and co-polarized beams as discussed in Sec. III-C.

B. Behavior over FoV

In the previous subsection, we assessed the performance of the bi-scalar beamformer at the beam centers. Another concern is the behavior of the PAF voltage beams over their respective FoVs, since the image processing should correct for this response. Figure 9 therefore shows $|J_{12}|$ for the optimal method and the bi-scalar method over the FoV at 1.42 GHz. This shows that both beamformers suffer from the direction dependent polarimetric response of the two feed systems, but that the optimal beamformer does a better job at the beam centers of the compound beams towards the edges of the FoV. For the optimal beamformer, there is always a small region around the beam center in which the instrumental crosspolarization is less than -45 dB while the bi-scalar beamformer produces some beams with -30 dB crosspolarization in their field centers. This can be explained by the fact that the bi-scalar beamformer relies on the intrinsic polarimetric

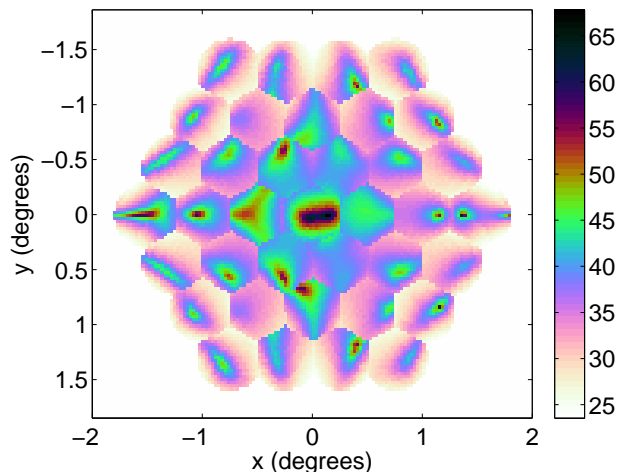


Fig. 10. IXR (in dB) for all 37 beams produced by the APERTIF system.

orthogonality between the two sets of orthogonally oriented antenna elements, which works very well in bore sight (the central beam), but deteriorates towards the edges of the FoV.

The results shown in Fig. 9 indicate that an appropriate correction for the polarimetric response of each PAF voltage beam is required in the image processing to reconstruct the polarimetric properties of the incident waves regardless of the beamforming approach used. The reconstructability of the polarization state of the received signals is measured by the IXR, which is shown in Fig. 10 for the bi-scalar beamformer. The simulations indicate that the inner 7 beams have an IXR better than 40 dB over almost their entire beam area, while the compound beams at the edges of the FoV still have an IXR of at least 25 dB. This gives an upper limit on the increase in the relative measurement error on the Stokes vector of 4% and 22% for the central beams and for the edges of the FoV respectively as predicted by (17). This should be sufficient to allow accurate reconstruction of polarized signals with limited sensitivity reduction due to image processing.

VI. CONCLUSIONS

In this paper we discussed the polarimetric and sensitivity performance of calibration schemes that exploit an unpolarized reference source. We demonstrated that the eigenvector method is sensitivity equivalent to the optimal beamformer. This implies that the eigenvector methods can exactly reproduce the result obtained from the optimal beamformer with an additional polarimetric correction after beamforming.

We have demonstrated that the eigenvector method is not suitable for use in an actual system without additional correction, because this method ignores the unitary ambiguity intrinsic to calibration on an unpolarized source. This ambiguity needs to be resolved either by imposing additional constraints on the system response, such as relying on the intrinsic polarimetric orthogonality between the feeds, or by additional calibration observation on two distinctly polarized sources.

The bi-scalar beamformer is not sensitivity equivalent to the optimal beamformer and relies on the intrinsic polarimetric

orthogonality of the feeds, but is easiest to implement in an actual system. We demonstrated that the bi-scalar beamformer can emulate the response of the optimal beamformer by forming cross- and co-polarized beams at the cost of halving the available beamforming bandwidth. We assessed the sensitivity loss and polarimetric performance of the bi-scalar beamformer using simulations for the APERTIF system, a PAF system currently being designed for the Westerbork Synthesis Radio Telescope. These simulations indicate that the sensitivity loss is about 4.5% while the typical IXR in the beam centers is about 38 dB. Since the bi-scalar beamformer relies on the polarimetric orthogonality of the feeds, the gradient of this orthogonality over the FoV causes variations in polarimetric response away from the beam centers that should be corrected for in the image processing. The simulations suggest that the IXR is at least 25 dB over the entire FoV, indicating that reconstruction of the polarimetric state of the incident wave should be possible with at most 22% increase in the relative error in the reconstructed image parameters. Since this is considered acceptable, our analysis indicates that XPD values as low as 20 dB inside the FoV are still acceptable, which is an important design requirement for future instruments like the SKA.

VII. ACKNOWLEDGMENT

The authors would like to thank Jaap Bregman, Wim van Cappellen, Johan Hamaker and Taylor Webb for their useful comments on earlier versions of this paper and Oleg Iupikov for his help in building the simulation required to simulate a phased array feed system.

APPENDIX

The condition number of a Jones matrix \mathbf{J} can be computed as

$$\kappa(\mathbf{J}) = \frac{\sigma_{\max}(\mathbf{J})}{\sigma_{\min}(\mathbf{J})} = \left(\frac{\lambda_{\max}(\mathbf{J}^H \mathbf{J})}{\lambda_{\min}(\mathbf{J}^H \mathbf{J})} \right)^{1/2}, \quad (43)$$

where $\sigma(\mathbf{J})$ denotes the singular value of \mathbf{J} indicated by the subscript and $\lambda(\mathbf{J}^H \mathbf{J})$ denotes the eigenvalue of $\mathbf{J}^H \mathbf{J}$ indicated by the subscript. Using \mathbf{J}_{eig} as given by (37) and solving for the characteristic polynomial, we find

$$\lambda_{\max} = \cos^2(\phi/2) \quad \text{and} \quad \lambda_{\min} = \sin^2(\phi/2), \quad (44)$$

such that

$$\kappa(\mathbf{J}_{\text{eig}}) = \frac{\cos(\phi/2)}{\sin(\phi/2)}. \quad (45)$$

Substitution of this result in (16) and a little algebraic manipulation gives (40).

REFERENCES

- [1] H. A. Zebker and J. J. van Zyl, "Imaging Radar Polarimetry: A Review," *Proceedings of the IEEE*, vol. 79, no. 11, pp. 1583–1606, Nov. 1991.
- [2] R. Touzi and M. Shimada, "Polarimetric PALSAR Calibration," *IEEE Transactions on Geoscience and Remote Sensing*, vol. 47, no. 12, pp. 3951–3959, Dec. 2009.
- [3] P. E. Dewdney, P. J. Hall, R. T. Schilizzi, and T. J. L. W. Lazio, "The Square Kilometre Array," *Proceedings of the IEEE*, vol. 97, no. 8, pp. 1482–1496, Aug. 2009.
- [4] M. de Vos, A. W. Gunst, and R. Nijboer, "The LOFAR Telescope: System Architecture and Signal Processing," *Proceedings of the IEEE*, vol. 97, no. 8, pp. 1431–1437, Aug. 2009.
- [5] W. A. van Cappellen and L. Bakker, "APERTIF: Phased Array Feeds for the Westerbork Synthesis Radio Telescope," in *IEEE International Symposium on Phased Array Systems and Technology*, Waltham (MA), USA, 12–15 Oct. 2010, pp. 640–647.
- [6] D. R. De Boer *et al.*, "Australian SKA Pathfinder: A High-Dynamic Range Wide-Field of View Survey Telescope," *Proceedings of the IEEE*, vol. 97, no. 8, pp. 1507–1521, Aug. 2009.
- [7] S. W. Ellingson *et al.*, "The Long Wavelength Array," *Proceedings of the IEEE*, vol. 97, no. 8, pp. 1421–1430, Aug. 2009.
- [8] A. R. Thompson, J. M. Moran, and G. W. Swenson Jr., *Interferometry and Synthesis in Radio Astronomy*, 2nd ed. Weinheim, Germany: Wiley-VCH Verlag GmbH, 2004.
- [9] K. F. Warnick, M. V. Ivashina, S. J. Wijnholds, R. Maaskant, and B. D. Jeffs, "Polarimetry with Phased Array Antennas: Theoretical Framework and Definitions," *IEEE Transactions on Antennas and Propagation*, vol. 60, no. 1, pp. 184–196, Jan. 2012.
- [10] B. Veidt *et al.*, "Demonstration of a Dual-Polarized Phased-Array Feed," *IEEE Transactions on Antennas and Propagation*, vol. 59, no. 6, pp. 2047–2057, Jun. 2011.
- [11] J. E. Roy and L. Shafai, "Generalization of the Ludwig-3 Definition for Linear Copolarization and Cross Polarization," *IEEE Transactions on Antennas and Propagation*, vol. 49, no. 6, pp. 1006–1010, Jun. 2001.
- [12] H. L. van Trees, *Optimum Array Processing*. New York, USA: John Wiley & Sons, Inc., 2002.
- [13] T. D. Carozzi and G. Woan, "A Fundamental Figure of Merit for Radio Polarimeters," *IEEE Transactions on Antennas and Propagation*, vol. 59, no. 6, pp. 2058–2065, Jun. 2011.
- [14] J. P. Hamaker, "Understanding radio polarimetry - IV. The full-coherency analog of scalar self-calibration: Self-alignment, dynamic range and polarimetric fidelity," *Astronomy & Astrophysics Supplement Series*, no. 143, pp. 515–534, May 2000.
- [15] —, "Understanding radio polarimetry - V. Making matrix self-calibration work: processing of a simulated observation," *Astronomy & Astrophysics*, vol. 456, no. 1, pp. 395–404, Sep. 2006.
- [16] S. J. Wijnholds, W. van Cappellen, and M. V. Ivashina, "Performance Assessment of Bi-scalar Beamformers in Practical Phased Array Feed Systems," in *Proceedings of the XXXth General Assembly and Scientific Symposium of the International Union of Radio Science (URSI GASS)*, Istanbul, Turkey, 13–20 Aug. 2011.
- [17] R. Maaskant, "Analysis of large antenna systems," Ph.D. dissertation, Eindhoven University of Technology, Eindhoven, The Netherlands, 2010.
- [18] M. V. Ivashina, O. Iupikov, R. Maaskant, W. A. van Cappellen, and T. Oosterloo, "An Optimal Beamforming Strategy for Wide-Field Surveys With Phased-Array-Fed Reflector Antennas," *IEEE Transactions on Antennas and Propagation*, vol. 59, no. 6, pp. 1864–1875, Jun. 2011.



Stefan J. Wijnholds (S06-M10-SM'12) was born in The Netherlands in 1978. He received the M.Sc. degree in astronomy and the M.Eng. degree in applied physics (both cum laude) from the University of Groningen, The Netherlands, in 2003, and the Ph.D. degree (cum laude) from Delft University of Technology, Delft, The Netherlands, in 2010.

After his graduation in 2003, he joined the R&D Department, ASTRON, the Netherlands Institute for Radio Astronomy, Dwingeloo, The Netherlands, where he works with the system design and integra-

tion group on the development of the next generation of radio telescopes. From 2006 to 2010, he was also affiliated with the Delft University of Technology, Delft, The Netherlands. His research interests lie in the area of array signal processing, specifically calibration and imaging, and system design of the next generation of radio telescopes.

Dr. Wijnholds received travel grants for the URSI GASS 2008 in Chicago (Ill.), the Asia-Pacific Radio Science Conference in Toyama, Japan (2010) and the URSI GASS 2011 in Istanbul, Turkey.



Marianna V. Ivashina (M11) received a Ph.D. in Electrical Engineering from the Sevastopol National Technical University (SNTU), Ukraine, in 2000. From 2001 to 2004 she was a Postdoctoral Researcher and from 2004 till 2010 an Antenna System Scientist at The Netherlands Institute for Radio Astronomy (ASTRON). During this period, she carried out research on an innovative Phased Array Feed (PAF) technology for a new-generation radio telescope, known as the Square Kilometer Array (SKA). The results of these early PAF projects

have led to the definition of APERTIF - a PAF system that is being developed at ASTRON to replace the current horn feeds in the Westerbork Synthesis Radio Telescope (WSRT). Dr. Ivashina was involved in the development of APERTIF during 2008-2010 and acted as an external reviewer at the Preliminary Design Review of the Australian SKA Pathfinder (ASKAP) in 2009. In 2002, she also stayed as a Visiting Scientist with the European Space Agency (ESA), ESTEC, in the Netherlands, where she studied multiplebeam array feeds for the satellite telecommunication system Large Deployable Antenna (LDA).

Dr. Ivashina received the URSI Young Scientists Award for the GA URSI, Toronto, Canada (1999), an APS/IEEE Travel Grant, Davos, Switzerland (2000), the 2nd Best Paper Award (Best team contribution) at the ESA Antenna Workshop (2008) and the International Qualification Fellowship of the VINNOVA - Marie Curie Actions Program (2009) and The VR project grant of the Swedish Research Center (2010). She is currently a Senior Scientist at the Department of Earth and Space Sciences (Chalmers University of Technology). Her interests are wideband receiving arrays, antenna system modeling techniques, receiver noise characterization, signal processing for phased arrays, and radio astronomy.



Rob Maaskant (M'11) was born in the Netherlands on April, 14th, 1978. He received his M.Sc. degree (*cum laude*) in 2003, and his Ph.D. degree (*cum laude*) in 2010, both in Electrical Engineering from the Eindhoven University of Technology. His Ph.D. has been awarded 'the best dissertation of the Electrical Engineering Department, 2010'. From 2003–2010 he was employed as an antenna research scientist at the Netherlands Institute of Radio Astronomy (ASTRON). He is currently a postdoctoral researcher in the Antenna Group at the Chalmers University of

Technology, Sweden, for which he won a Rubicon postdoctoral fellowship from the Netherlands Organization for Scientific Research (NWO), 2010. He received the 2nd best paper prize ('best team contribution') at the 2008 ESA/ESTEC workshop, Noordwijk, and was awarded a Young Researcher grant from the Swedish Research Council (VR), in 2011. Dr. Maaskant is the primary author of the CAESAR software; an advanced integral-equation based solver for the analysis of large antenna array systems. His current research interest is in the field of receiving antennas for low-noise applications, meta-material based waveguides, and computational electromagnetics to solve these types of problems.



Karl F. Warnick (SM'04) received the B.S. degree (*magna cum laude*) with University Honors and the Ph.D. degree from Brigham Young University (BYU), Provo, UT, in 1994 and 1997, respectively.

From 1998 to 2000, he was a Postdoctoral Research Associate and Visiting Assistant Professor in the Center for Computational Electromagnetics at the University of Illinois at Urbana-Champaign. Since 2000, he has been a faculty member in the Department of Electrical and Computer Engineering at BYU, where he is currently a Professor. In 2005

and 2007, he was a Visiting Professor at the Technische Universität München, Germany. Dr. Warnick has published many scientific articles and conference papers on electromagnetic theory, numerical methods, remote sensing, antenna applications, phased arrays, biomedical devices, and inverse scattering, and is the author of the books *Problem Solving in Electromagnetics*, *Microwave Circuits*, and *Antenna Design for Communications Engineering* (Artech House, 2006) with Peter Russer, *Numerical Analysis for Electromagnetic Integral Equations* (Artech House, 2008), and *Numerical Methods for Engineering: An Introduction Using MATLAB and Computational Electromagnetics Examples* (Scitech, 2010).

Dr. Warnick was a recipient of the National Science Foundation Graduate Research Fellowship, Outstanding Faculty Member award for Electrical and Computer Engineering (2005), and the BYU Young Scholar Award (2007). He has served the Antennas and Propagation Society as a member of the Education Committee and as a session chair and special session organizer for the International Symposium on Antennas and Propagation and other meetings affiliated with the Society. He is a frequent reviewer for the IEEE Transactions on Antennas and Propagation and Antennas and Wireless Propagation Letters. Dr. Warnick has been a member of the Technical Program Committee for the International Symposium on Antennas and Propagation for several years and served as Technical Program Co-Chair for the Symposium in 2007.